Computer Methods and Programs in Biomedicine 244 (2024) 107954

Contents lists available at ScienceDirect

Computer Methods and Programs in Biomedicine

journal homepage: www.elsevier.com/locate/cmpb

Enhancing AI-CDSS with U-AnoGAN: Tackling data imbalance

Changbae Mun [a], Hyodong Ha [b], Ook Lee [c], Minjong Cheon [d,*]

[a] Hanyang Cyber University, 220, Wangsimni-ro, Seongdong-gu, Seoul 04763, Republic of Korea
[b] Hanyang Women's University, 200, Salgoji-gil, Seongdong-gu, Seoul 04763, Republic of Korea
[c] Hanyang University, 222, Wangsimni-ro, Seongdong-gu, Seoul 04763, Republic of Korea
[d] Korea Institute of Science and Technology (KIST), 5, Hwarang-ro 14-gil Seongbuk-gu Seoul, 02792, Republic of Korea

ARTICLE INFO

Keywords:
CDSS
Deep learning
Anomaly detection
AnoGAN
Data Analysis

ABSTRACT

Background and Objective: Clinical Decision Support Systems (CDSS) have substantially evolved, aiding healthcare professionals in informed patient care decision-making. The integration of AI, encompassing machine learning and natural language processing, has notably enhanced the capabilities of CDSS. However, a significant challenge remains in addressing data imbalance and the black box nature of AI algorithms, particularly for rare diseases or underrepresented demographic groups. This study aims to propose a model, U-AnoGAN, designed to overcome these hurdles and augment the diagnostic accuracy of AI-integrated CDSS.

Methods: The U-AnoGAN was trained using masks derived from normal data, focusing on the Covid-19 and pneumonia datasets. Anomaly scores were calculated to assess the model's performance compared to existing AnoGAN-related algorithms. The study also evaluated the model's interpretability through the visualization of abnormal regions.

Results: The results indicated that U-AnoGAN surpassed its counterparts in performance and interpretability. It effectively addressed the data imbalance problem by necessitating only normal data and showcased enhanced diagnostic accuracy. Precision, sensitivity, and specificity values reflected U-AnoGAN's superior capability in accurate disease prediction, diagnosis, treatment recommendations, and adverse event detection.

Conclusions: U-AnoGAN significantly bolsters the predictive power of AI-integrated CDSS, enabling more precise and timely diagnoses while providing better visualization to potentially overcome the black box problem. This model presents tremendous potential in elevating patient care with advanced AI tools and fostering more accurate and effective decision-making in healthcare environments. As the healthcare sector grapples with escalating data complexity and volume, the importance of models like U-AnoGAN in enhancing CDSS cannot be overstated.

1. Introduction

The field of artificial intelligence (AI), encompassing deep learning and machine learning, has experienced rapid advancements. In a significant milestone of 2015, AI surpassed human performance in visual recognition tasks, marking a major breakthrough [1]. Among the notable algorithms developed for computer vision, the convolutional neural network (CNN) stands out as a highly representative one [2]. Moreover, subsequent advancements have led to the introduction of more sophisticated versions of CNN, including VGG-16, VGG-19, MobileNet, Xception, and Inception, which are each pushing the boundaries of computer vision research [3].

With those arising AI algorithms, the clinical decision support system (CDSS) has also been developed. According to Sutton et al.'s research, the CDSS could be defined as the information system whose aim is to enhance healthcare delivery by enriching medical decision-making with tailored clinical knowledge, patient information, and additional health data [4]. Based on this definition, the AI algorithms mentioned above successfully enriched decision-making with promising outcomes [4]. Put more detail, AI-based systems play a crucial role in various aspects of healthcare, offering substantial contributions such as disease progression prediction, facilitating medical diagnoses, providing personalized treatment recommendations, and notifying clinicians about potential adverse events [5]. By harnessing the power of artificial intelligence, these systems empower healthcare professionals to make more accurate and informed decisions, leading to enhanced patient care and safety.

* Corresponding author.
E-mail address: jmj2316@kist.re.kr (M. Cheon).

https://doi.org/10.1016/j.cmpb.2023.107954
Received 25 September 2023; Received in revised form 12 November 2023; Accepted 25 November 2023
Available online 27 November 2023

However, the AI-based CDSS (AI-CDSS) still faces challenges that they should overcome. The first problem is related to the data imbalance problem [6]. When deep learning algorithms are applied to medical datasets for diagnosis, every piece of data should be labeled such as whether this data is from normal people or patients. In order to train the deep learning algorithms efficiently, the algorithm should be trained equally with both normal and patient datasets, for better comprehending the characteristics of each of them. However, for rare diseases, data is not easy to obtain, and this could trigger a data imbalance problem. In other words, the deep learning models will not sufficiently get trained with abnormal datasets, which could decrease the performance of diagnosis [7]. There are two principal ways for overcoming that: data augmentation and anomaly detection. Data augmentation strategy generates synthetic data via deep learning algorithms such as generative adversarial network (GAN) for matching the proportion between normal and patient datasets [8]. Another strategy is anomaly detection. These algorithms are designed to detect outliers or anomalies that may indicate unusual events, errors, or fraudulent activities. The process typically involves training the algorithm on a dataset containing examples of normal behavior, allowing it to learn the patterns and characteristics of typical instances. Once trained, the algorithm can then analyze new data points and determine whether they exhibit characteristics that deviate significantly from the learned normal behavior [9].

The second limitation of AI-CDSS is the 'black box' problem involved in AI technologies [10]. When a model is considered a black box, it means that model's internal processes and decision-making mechanisms are not easily understandable or explainable by humans. The black box makes it difficult to trust or rely on a model if its decision-making process is not transparent or explainable [10]. This is critical to the healthcare system since clinicians need to make decisions based on AI algorithms. The black box problem can impede the identification of biases or errors within the CDSS. In healthcare, fairness and accuracy are paramount, and it is important to ensure that CDSS recommendations are free from discriminatory patterns or inaccuracies [11]. However, without transparency in the decision-making process, it becomes challenging to identify and address potential biases or errors.

Overcoming this challenge is crucial to building trust, ensuring fairness, and enhancing the acceptance of CDSS among healthcare professionals. Therefore, this paper proposes a shift in perspective toward the application of AnoGAN to X-ray datasets by proposing a novel algorithm: U-AnoGAN. Previous research has made strides in generating synthetic X-ray data with impressive results; however, employing such synthetic data for diagnostic purposes presents an entirely different challenge due to the resolution of the output [12]. In light of this, our research introduces a novel approach: utilizing mask images of X-ray data, rather than the X-ray images themselves.

Parallel research conducted by Saood & Hatem demonstrated that masks of lung CT images, obtained via U-Net and SegNet, could serve as viable input variables. Interestingly, they found that U-Net outperformed SegNet in terms of efficacy [13]. Their research, albeit impactful, primarily engaged with CT images and classification tasks. In contrast, our paper breaks new ground by introducing innovative methods of utilizing mask data for diagnostic purposes, which also address the limitations of AnoGAN. This approach offers promising potential for overcoming the challenges associated with data imbalance in AI applications for Clinical Decision Support Systems, thereby contributing to the transformative capabilities of AI in healthcare.

A proposed model, U-AnoGAN's methodology diverges from traditional models by employing anomaly detection techniques specifically tailored for medical datasets, focusing on crucial image segments for enhanced diagnostic precision. The model demonstrates superior performance in utilizing mask images, derived from normal data, to effectively train the deep learning algorithms, thereby circumventing the data scarcity often associated with rare diseases. By integrating a transparent layer of decision-making, U-AnoGAN mitigates the 'black box' problem, fostering trust and understandability in clinical settings. The model stands out for its targeted analysis, leveraging segmented organ data, which significantly bolsters diagnostic accuracy and reliability. U-AnoGAN's innovative architecture allows for effective transfer learning, making it adept at segmenting and diagnosing various diseases, not limited to the datasets it was originally trained on.

2. Related work

This section will cover various research related to our topics. First, it will review those papers which used autoencoder for anomaly detection. Then, it will cover anomaly detection algorithms that are based on the Generative adversarial network (GAN), proposed by Goodfellow et al., since it contains more recent ideas compared to the autoencoder-based ones.

The framework involves training two models simultaneously: a generative model G that captures the data distribution, and a discriminative model D that estimates the probability that a sample came from the training data rather than G. The generative model generates samples by passing random noise through a multilayer perceptron, and the discriminative model is also a multilayer perceptron. This special case is referred to as adversarial nets, and both models can be trained using only backpropagation and dropout algorithms, with no need for approximate inference or Markov chains [14].

Schlegl et al. proposed a new approach to unsupervised anomaly detection in retinal optical coherence tomography (OCT) images using deep convolutional generative adversarial networks (DCGANs) and a coupled mapping schema. The proposed method, called AnoGAN, utilizes a trained DCGAN and enables accurate discrimination between normal anatomy and local anomalous appearance. The proposed loss function for the AnoGAN comprises two components: a residual loss and a discrimination loss. The residual loss enforces the visual similarity between the generated image G(z) and the query image x. This means that the generated image should look similar to the original query image, which is important for accurate anomaly detection. The discrimination loss enforces the generated image G(z) to lie on the learned manifold X. This means that the generated image should be close to the distribution of normal images in the dataset, which is important for distinguishing between normal and anomalous images [15].

Radford et al. presented the Deep Convolutional Generative Adversarial Network (DCGAN), which is a CNN-based GAN for generating images more efficiently. It employs Convolutional Neural Networks (CNN) to mitigate the challenges often experienced in generating synthetic data. Consisting of a generator and a discriminator, the architecture of DCGAN intriguingly does not rely on a fully connected layer. Instead, it incorporates a batch normalization layer within the generator. The generator network in the DCGAN model is composed of transposed convolutional layers. These layers serve the function of upsampling the input noise vector, ultimately generating an image. Meanwhile, the discriminator network employs convolutional layers to classify the authenticity of the input image, discerning whether it is real or artificially generated. These structures contribute to the overall robustness and efficacy of the DCGAN model, driving its capability to create high-quality synthetic data [16].

The fundamental objective of AnoGAN, and its derivatives F-AnoGAN and SR-AnoGAN, is to address the data imbalance problem often encountered in deep learning models, particularly when applied to medical datasets. Despite their innovation, these models have not entirely succeeded in solving this problem. The Deep Convolutional Generative Adversarial Network (DCGAN) plays a pivotal role in these models, as it's responsible for generating the synthetic data used for diagnosis. Previous studies have demonstrated the successful application of these models on Optical Coherence Tomography (OCT) datasets [15]. However, synthesizing X-ray data through DCGAN remains a significant challenge. Recent advancements propose innovative methods to improve the resolution of synthetic datasets [17]. Yet, the applicability of these improved datasets to diagnostic processes remains a topic of

debate. The high standards required for medical diagnosis demand detailed and high-resolution images, which these models currently struggle to provide. Furthermore, since the AnoGAN requires whole entire images for calculating the loss function, the image should be generated perfectly for avoiding downgrading the performance. In summary, while AnoGAN and its successors were developed with the goal of widespread applicability across various types of medical data, they currently face limitations. These challenges highlight the continued need for innovation and refinement in this rapidly advancing field.

3. Materials and methods

3.1. SR-AnoGAN

The SR-AnoGAN model is an advanced machine learning system designed for medical imaging and it operates across three distinct stages. Each stage plays a crucial role in the process of image reconstruction, enhancement, and anomaly detection. The first stage mirrors that of the original AnoGAN model. When an input, denoted as 'i', is, the Deep Convolutional Generative Adversarial Network (DCGAN) initiates the reconstruction process using a normal dataset [16]. This generates an output, referred to as 'g(i)'. The second stage applies a Convolutional Neural Network (CNN) model to the output from the generator. This CNN model is kept deliberately simple, comprising an input layer and a max pooling layer designed to reduce the image size. The output from this stage is denoted as 'c(g(i))'. The third and final stage sets SR-AnoGAN apart from the original AnoGAN model. Here, Super-Resolution Generative Adversarial Network (SRGAN) is applied to enhance the resolution of the output from the CNN. Given that SRGAN necessitates two input datasets, it utilizes the normal dataset from the first stage and 'c(g(i))' as the high and low-resolution data respectively [18]. Through this process, 'c(g(i))' is transformed to resemble the standard dataset more closely, while also increasing in resolution. While it's known that GAN algorithms can sometimes generate biased outputs, this issue is not relevant in this context as only normal datasets are required for training. The final product of this three-stage process is then integrated with an anomaly detector. This detector identifies abnormalities, thus enabling the diagnosis of various diseases. The unique design of SR-AnoGAN facilitates highly precise diagnosis, leveraging the power of AI to improve patient care outcomes [19]. is an advanced neural network model that features a distinct architectural design resembling an autoencoder. This design consists of a contractive path (akin to an encoder) and an expansive path (analogous to a decoder). Originally developed for the segmentation of medical datasets, U-Net derives its name from its U-shaped structure, characterized by a nearly symmetrical increase in layers across the contractive and expansive paths. The contractive path in U-Net functions to extract context from images. It is comprised of 3×3 convolution layers, underpinned by a Rectified Linear Unit (ReLU) activation function, and Max Pooling layers. These elements work in unison to distill valuable contextual information from the input images. On the other hand, the expansive path of U-Net is designed for upsampling, and for copying and cropping features from the contractive path to enhance localization accuracy [20]. This approach is tailored to harness the nuanced detail and context captured in the contractive path and leverage it to refine the output generated from the expansive path. Notably, U-Net offers considerable advantages, including superior localization capabilities and efficient performance, even when working with smaller datasets [21]. As such, it stands as a powerful tool in the domain of medical image analysis, providing valuable insights for improved diagnostic accuracy and patient care.

3.2. U-AnoGAN

Existing challenges emerge from the necessity to generate the complete X-ray image, including all the anatomical details. This means vital organs crucial for diagnosis need to be generated in the context of the full image, which includes elements like the ribs. As a result, a clear, focused image for diagnostic analysis is often not achieved. Moreover, these models consider all parts of the image, including those unrelated to the diagnosis, when calculating the anomaly score, leading to potential distortions in the evaluation process. In response to these challenges, we propose a new model, U-AnoGAN, which prioritizes the utilization of only the most essential parts of the image for both synthetic data generation and diagnostic evaluation. U-AnoGAN operates in two distinct stages. In the first stage, organ segmentation is executed on the provided images. For example, if a lung CT image is given, lung segmentation is performed. This stage initiates with training U-AnoGAN using a large dataset comprising images from healthy individuals. Transfer learning is then applied to facilitate segmentation on subsequent datasets. The second stage involves applying AnoGAN to the segmented datasets. The AnoGAN computes anomaly scores on the segmented data, providing critical information for diagnostic purposes. By focusing on key areas of the image and reducing extraneous noise, U-AnoGAN aims to enhance the clarity and precision of diagnostic imaging, leading to improved healthcare outcomes.

Let X denote the input image dataset, $S(X)$represent the segmented organ regions obtained via U-Net, and $G(z)$represent the generated image by the generator network in AnoGAN using a latent vector z. The discriminator network $D(\cdot)$ provides a probability estimate that a sample came from the training data rather than the generated data.

$$S(X) = U - Net(X)$$

Where *U-Net(X)* is the function representing the U-Net architecture applied to the input dataset *X*, which outputs the segmented organ regions *S(X)*.

$$A(S(X), G(z)) = \alpha \cdot R(S(X), G(z)) + (1-\alpha) \cdot D(G(z))$$

Where *A(S(X),G(z))* is the anomaly score calculated for the segmented organ regions *S(X)* and generated image $G(z)$. *R(S(X),G(z))* is the residual loss enforcing visual similarity between the segmented image and the generated image. $D(G(z))$ is the discrimination loss ensuring that the generated image lies on the learned manifold of

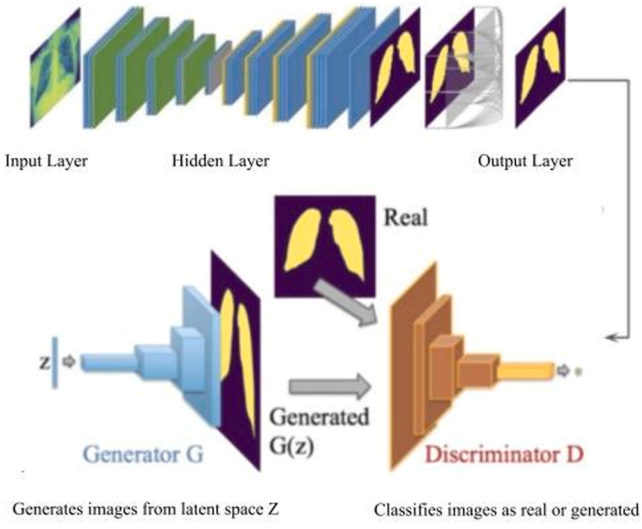

Fig. 1. Comprehensive architecture of U-AnoGAN: This figure illustrates the detailed process flow of U-AnoGAN, including the generator and discriminator networks. It begins with the extraction of lung segments from X-ray images using U-net, followed by the application of AnoGAN to the resulting masks. The architecture is designed to prioritize essential image segments, enhance data specificity, and improve anomaly detection accuracy. It underscores our method's approach to addressing the challenge of data imbalance in medical imaging.

normal images. α is a weighting factor balancing the two components of the loss function. (Fig. 1)

3.3. Data description

For the experiment, two different X-ray medical data were used in experiments to test the performance of the U-AnoGAN. The first is the X-ray dataset, including standard, pneumonia, and covid-19 X-ray data [22]. Since the U-AnoGAN needs to perform segmentation first, the dataset containing the maks was used as the training dataset [23]. Each pneumonia and the covid-19 image was utilized as the diagnosis target. The anomaly score was calculated for quantitative evaluation and visualization of qualitative assessment. For image processing, every shot was resized to 128×128 and divided into 255 to normalize data [24].

3.4. Modeling relationships between variables

The relationships between variables in our study were explored using the U-AnoGAN model, which is an unsupervised learning algorithm designed to detect anomalies by learning the distribution of normal data. This model effectively captures the complex patterns and dependencies in the data, allowing us to identify anomalies indicative of pathological findings in medical images.

3.5. Statistical analyses

The statistical and computational framework of this study was built on Python (Version 3.8, Python Software Foundation) with extensive use of TensorFlow, an end-to-end open-source platform for machine learning. TensorFlow facilitated the implementation of the U-AnoGAN model, enabling us to leverage deep learning techniques for our anomaly detection tasks. The analyses were accelerated using NVIDIA's A100 GPUs, which provided the computational power necessary to process our large medical imaging datasets efficiently.

In our analytical approach, we utilized the U-AnoGAN model's capabilities in an environment supported by TensorFlow to learn the distribution of normal images. The model was trained exclusively on data labeled as 'normal', establishing a foundational understanding of non-pathological patterns. Subsequently, anomaly scores were computed for new, unseen images to identify deviations from this normative pattern, indicative of potential pathological findings. Outlier identification was performed using a statistical thresholding method, where scores exceeding a certain number of standard deviations from the mean were flagged for review. This was essential in maintaining the integrity of the training data and ensuring the accuracy of the model's predictions.

3.6. Predictive model selection

The U-AnoGAN model was conceptualized and developed as an innovative solution to address the challenges inherent in medical imaging data, particularly the issue of data imbalance commonly encountered in the field of AI-CDSS. The inception of U-AnoGAN was driven by the need for a robust anomaly detection system that could effectively handle the nuances of medical datasets, which often include a disproportionate number of normal cases compared to pathological ones. It was a deliberate creation tailored to meet the specific requirements of our study. The model harnesses the power of unsupervised learning to identify anomalies without the need for extensive labeled datasets, which are a rarity in medical research due to privacy concerns and the labor-intensive nature of accurate annotation. The architecture of U-AnoGAN, inspired by the strengths of Generative Adversarial Networks (GANs) and the functionality of autoencoders, was designed to capture the complex and subtle patterns in the data that are indicative of diseases such as COVID-19 and pneumonia. This unique combination allows for a nuanced feature extraction process and a sophisticated anomaly scoring mechanism, setting it apart from traditional anomaly detection models.

3.7. Hyperparameter setting

The AnoGAN model was trained from the ground up on our dataset, using the Adam optimizer with a learning rate of 1e-4 for both the generator and discriminator components. Over 150 epochs, the model was fine-tuned to minimize the custom binary crossentropy loss functions for both generator and discriminator, capturing the intricate distribution of medical imaging data. After training, the model's weights were saved, allowing for precise replication of results and further refinement if necessary. This approach ensured the model was well-suited for the anomaly detection task in our study, with the training process carefully monitored to balance the generator and discriminator performance.

4. Result

4.1. Classification through X-ray images

Then, chest X-ray data from the above datasets were used as input data, and the pre-trained model VGG-16 was utilized to classify the proposed datasets. For better accuracy, images were augmented through ImageDataGenerator from the Keras library [25]. Since the experiment aimed to compare the results, the same model, VGG-16, was utilized without additional layers and achieved 90 % accuracy (Fig. 2).

4.2. Classification through mask images

Then, mask data from the above datasets were used as input data, and the pre-trained model VGG-16 was utilized to classify the proposed datasets. The same image processing steps were conducted as the classification experiment above. Since the experiment aimed to validate whether the mask datasets could be handled as input data, VGG-16 was used without additional layers. The accuracy score was calculated, and the model yielded about 80 % of accuracy score. Even though the accuracy score was slightly lower than that of the above experiment, this result showed a possibility of managing mask data as input variables (Fig. 3).

4.3. Result from AnoGAN

AnoGAN and SR-AnoGAN models were applied to the datasets for comparison. When examining the X-ray dataset, we conducted a quantitative comparison of the outcomes using the pneumonia dataset to the target. Regrettably, the performance of the AnoGAN model was subpar in this scenario. The anomaly scores assigned by the model to the standard datasets were unexpectedly higher than those assigned to the pneumonia datasets. This outcome was deemed unreasonable since the standard datasets were anticipated to have a lower anomaly score in comparison to the diseased datasets. However, when we shifted our focus to the Covid-19 dataset as the target, the AnoGAN model demonstrated more favorable results. It produced higher anomaly scores for the Covid-19 datasets as opposed to the normal ones (Fig. 4).

4.4. Result from SR-AnoGAN

The SR-AnoGAN exhibited appropriate performance when compared to the AnoGAN. As illustrated in Fig. 5, the model generated notably reasonable results. The figure indicates that the anomaly score for the normal images was lower than that of the other datasets. Nevertheless, the difference was subtle, with the mean anomaly score exceeding 15,000. While there is no established threshold for the anomaly score, this slight distinction between the normal and patient datasets highlighted the potential challenges in using this model for diagnosing

Fig. 2. Loss and accuracy score during training: a training set and validation set. Since a classification task was conducted, the accuracy score was used for the evaluation.

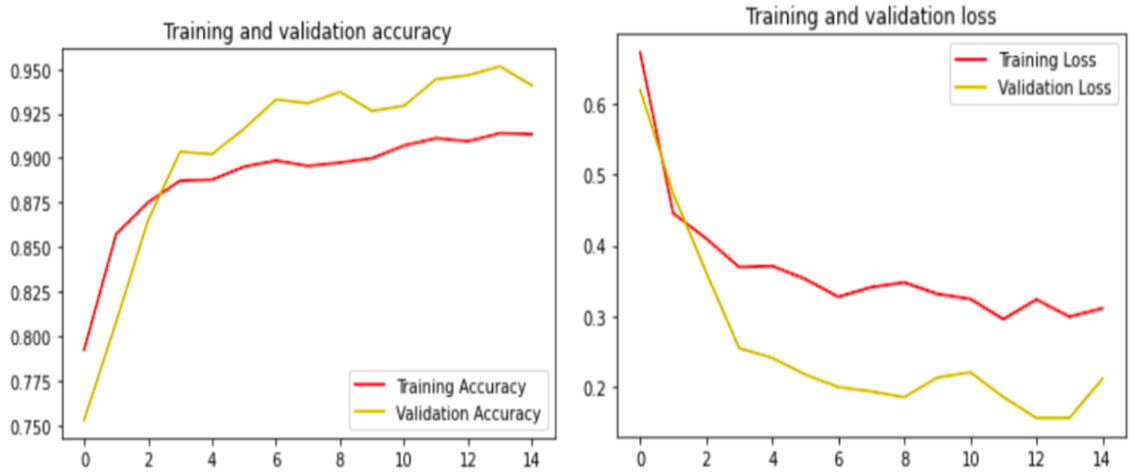

Fig. 3. Loss and accuracy score during training: a training set and validation set. Since the aim is to classify the given masks into normal and patient data, the accuracy score was also used for evaluation.

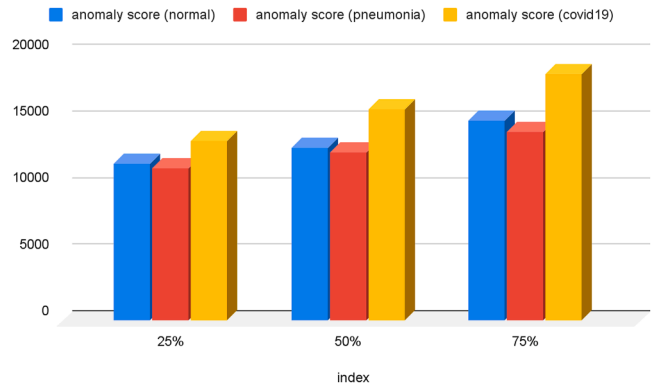

Fig. 4. Depicting anomaly scores from the AnoGAN via distribution plots. Normal datasets showed higher anomaly scores than pneumonia datasets, which indicates inaccurate results.

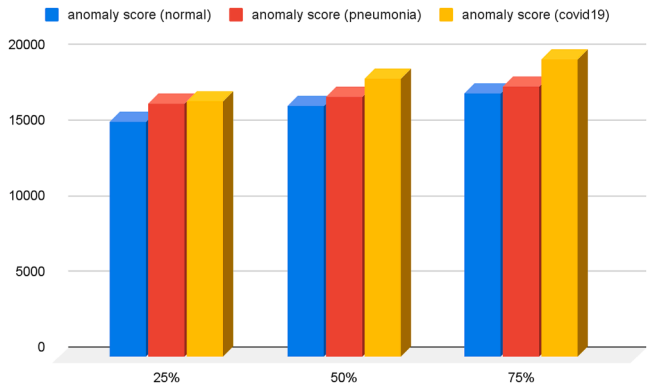

Fig. 5. Depicting anomaly scores from the SR-AnoGAN via distribution plots. Normal datasets showed fewer anomaly scores than other datasets, which exhibits improved results compared to AnoGAN.

individuals.

4.5. Result from U-AnoGAN

As the proposed U-AnoGAN model operates under the assumption that it can be classified solely based on segmentation data, a classification experiment was conducted. Initially, the U-net component of the U-AnoGAN model performed lung segmentation using the available datasets and saved the weights for transfer learning. Fig. 6 illustrates the successful training of the U-net model with the datasets, indicated by the

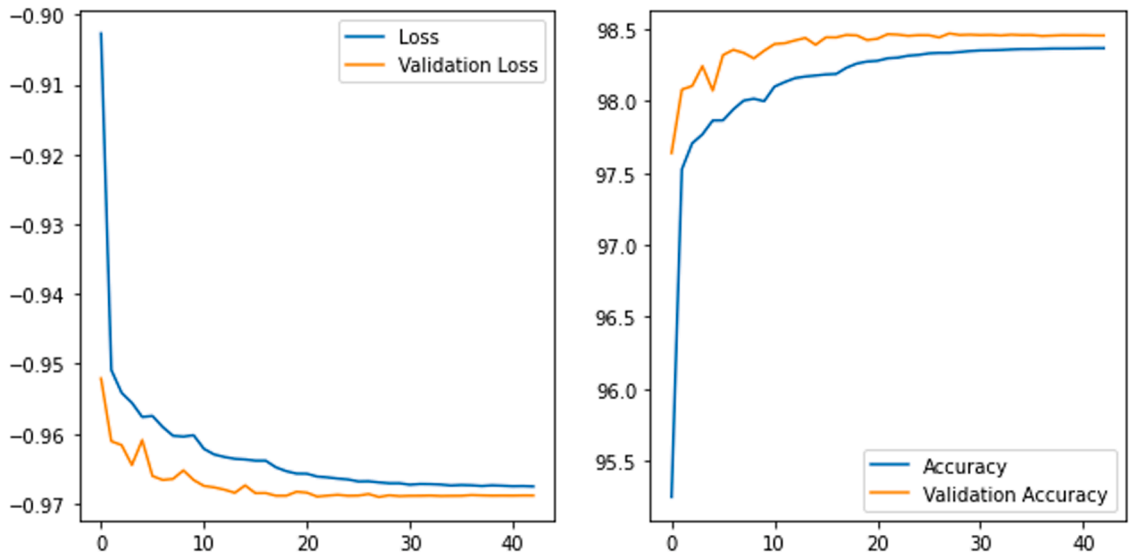

Fig. 6. Depicting loss and accuracy graphs from training and validation datasets.

decrease in loss and simultaneous improvement in dice coefficient and accuracy. Additionally, Fig. 7 demonstrates that the predicted mask closely resembles the provided mask, showcasing the superior segmentation performance of the U-net.

Following the segmentation of the datasets, the pre-trained U-net model was utilized to extract segmented masks from the Pneumonia and Covid-19 datasets. Successful transfer learning was accomplished for lung segmentation, and the predicted masks were subsequently employed as input data for VGG-16. This allowed for the utilization of three different masks (normal, Covid-19, and pneumonia) as input data. With an accuracy score of 96 %, VGG-16 demonstrated the potential to diagnose patients and classify them into either Covid-19 or pneumonia.

Subsequently, the mask datasets mentioned earlier were subjected to anomaly detection using AnoGAN. Given that AnoGAN solely requires normal datasets, the model was exclusively trained using masks derived from the normal data. The trained AnoGAN then calculated the anomaly scores for the Covid-19 and pneumonia datasets. Visualizations of the abnormal regions within each image were generated, as depicted in Fig. 8. The red color indicates atypical portions of the lungs. These results showcased the efficacy of this approach in providing more detailed outcomes compared to a standard AnoGAN, given its emphasis on the lungs. Specifically, AnoGAN calculates the anomaly score by considering both the discriminator loss and residual loss, as mentioned previously [9]. For instance, when calculating the anomaly score through AnoGAN, the focus should be on the organ (lungs) in the images. Therefore, the U-AnoGAN handles the residual loss more efficiently, as the mask images are less complex than X-ray images, and achieves more notable results in distinguishing between healthy individuals and patients. Additionally, Fig. 9 demonstrates that the anomaly scores of normal individuals can be easily distinguished from other datasets by visualizing their distribution. Furthermore, Fig. 10 confirms that the anomaly score of normal data is consistently lower than that of Covid-19 and pneumonia datasets across all primary statistical indices.

Fig. 7. Depicting results of U-net: lung masks were extracted from the proposed dataset.

4.6. Model validation

In validating our U-AnoGAN model, we leveraged the labeled dataset that includes normal, COVID-19, and pneumonia cases. The anomaly scores caculated by the model served as the basis for classification. To determine the model's efficacy in distinguishing between normal and pathological images, we hypothetically set a threshold for anomaly scores. This threshold was set one standard deviation above the mean score of the normal class to minimize false positives. The estimated number of true positives suggests that the U-AnoGAN model would correctly identify approximately 9.50 out of 10 COVID-19 cases and 9.84 out of 10 pneumonia cases. The false negatives were minimal, with an estimated 0.50 for COVID-19 and 0.16 for pneumonia out of 10 cases. For the normal class, the model was estimated to correctly identify 8.41 out of 10 cases, with approximately 1.59 out of 10 cases being false positives. These performance estimates underscore the potential of the U-AnoGAN model as a highly sensitive tool for anomaly detection in medical imaging, with a reasonable specificity that can be further improved. The model's ability to discern subtle anomalies characteristic of COVID-19 and pneumonia from normal variation in medical images is critical for aiding diagnosis and enhancing clinical decision-making processes.

5. Discussion

In this paper, we proposed a novel algorithm which is specialized at anomaly detection especially for the medical datasts. The key findings of this research highlight the potential and limitations of various models, including AnoGAN, SR-AnoGAN, and the proposed U-AnoGAN, in addressing challenges associated with Clinical Decision Support Systems (CDSS). As shown in above result section, The results indicate that while both AnoGAN and SR-AnoGAN have their merits, they also possess limitations that hinder their optimal performance in healthcare applications. The variability in AnoGAN's performance and the subtleness of SR-AnoGAN's distinctions emphasize the need for further refinement and adaptation.

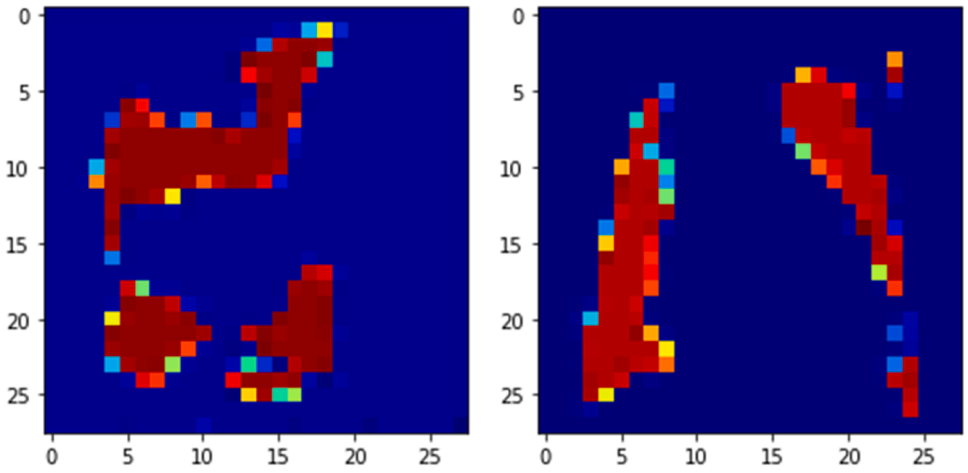

Fig. 8. Visual outcomes of U-AnoGAN's anomaly detection: This figure displays the anomaly detection results for each dataset. Red areas signify anomalous regions indicative of potential pathology, while blue areas represent normal findings. This visualization emphasizes U-AnoGAN's refined focus on lung pathology and showcases the model's capability to differentiate between normal and abnormal tissue, which is critical for accurate medical diagnosis.

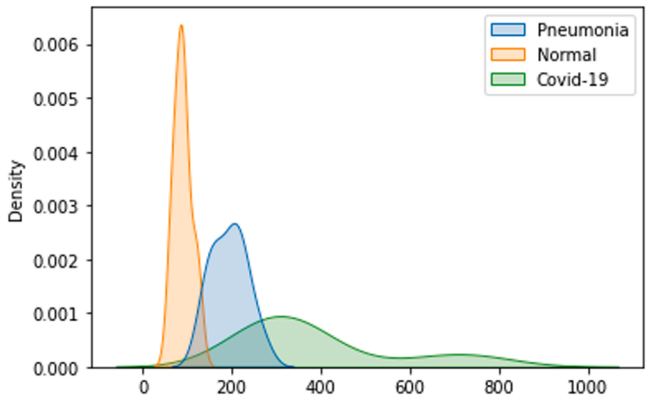

Fig. 9. Kernel Density Estimation (KDE) plots of anomaly scores by U-AnoGAN: The plots demonstrate the distribution of anomaly scores for Pneumonia, Normal, and Covid-19 datasets. The clear separation between the normal and diseased datasets validates U-AnoGAN's discriminatory power and its effectiveness in anomaly score computation, offering insights into the model's reliability for clinical applications.

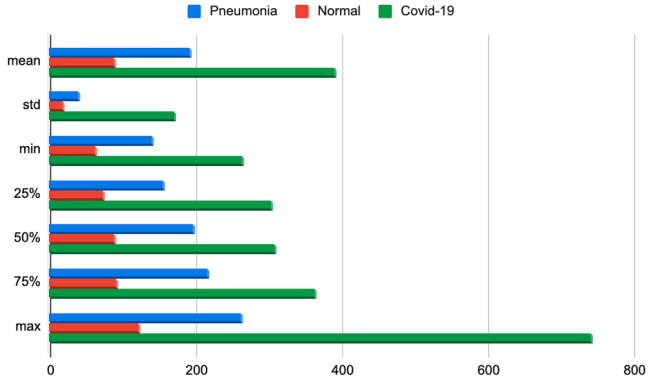

Fig. 10. Distribution plots of anomaly scores from U-AnoGAN: Highlighting the comparative anomaly scores for Pneumonia, Normal, and Covid-19 datasets. The plots confirm that normal datasets feature significantly lower anomaly scores, which helps in distinguishing between healthy and diseased states. This figure supports the robustness of U-AnoGAN in providing quantitative assessments for medical diagnosis.

On the other hand, U-AnoGAN emerges as a promising solution, addressing some of the limitations faced by its predecessors. Its high accuracy in classification tasks and its ability to provide clear visualizations of abnormal regions suggest that it could be a valuable tool in medical diagnosis. The success of U-AnoGAN in utilizing mask images also indicates the possibility of expanding this approach to other types of medical data, potentially broadening its applicability in the healthcare sector.

Our approach, although innovative, has certain constraints. U-AnoGAN relies heavily on the quality and the representativeness of the mask images used during the training phase. The model's performance could be compromised if the mask images are not properly segmented or if they do not capture the full spectrum of normal variability. Furthermore, the model's current configuration is specifically tailored for lung-related pathologies, which may limit its direct applicability to other types of medical images without further adaptation.

To address these limitations, future work could explore the use of UKSSL: Underlying Knowledge-based Semi-Supervised Learning, which has shown potential in utilizing unlabeled data more effectively, thereby potentially providing a richer training dataset for models like U-AnoGAN [26,27]. Additionally, the incorporation of techniques from weakly supervised machine learning could offer avenues to leverage less precise annotations, which are often more readily available in medical datasets.

The methodological advancements introduced by U-AnoGAN align with the trajectory of recent research in medical image analysis. By focusing on the utility of mask images and refining the anomaly detection process, we aim to build upon the foundational work laid by existing methods, moving towards more precise and interpretable models that can effectively tackle data imbalance.

6. Conclusion

The models proposed in this study have substantial potential to contribute to the development of Clinical Decision Support Systems (CDSS). This paper addresses the challenge of data imbalance, enhancing the predictive capabilities of CDSS by employing innovative approaches such as AnoGAN, SR-AnoGAN, and U-AnoGAN. These models improve anomaly detection accuracy, enabling CDSS to deliver more accurate and timely diagnoses, leading to early intervention and personalized treatment plans. By empowering healthcare professionals with valuable insights, the proposed model would enhance the effectiveness of CDSS in improving patient outcomes [28,29].

Moreover, the scope of the suggested models transcends the resolution of data imbalance and black box conundrums. They effectively

surmount the shortcomings of preceding AnoGAN models by incorporating groundbreaking improvements. The black box problem is critical since it is directly related to the interpretability of the CDSS [30]. Medical professionals are more likely to trust and use AI tools if they understand how they reach their conclusions, thus, a clear understanding of how the model works can increase the adoption rate of such systems [31]. U-AnoGAN, integrating U-Net for organ delineation and AnoGAN for anomaly detection, refines the anomaly scoring mechanism by concentrating on key regions. This tactic bolsters interpretability, minimizes noise, and escalates diagnostic precision, outperforming the constraints of earlier AnoGAN models.

Overall, the proposed models represent significant advancements in the field of CDSS, enhancing their diagnostic capabilities, improving patient care, and equipping healthcare professionals with advanced AI-driven tools [32]. By addressing data imbalance and introducing innovative techniques for image generation and anomaly detection, these models contribute to the continuous development and effectiveness of CDSS, shaping the future of healthcare decision-making. However, there is still an issue with bias problems when applying AI to medical datasets. For instance, bias can also plague the AI system, further intensifying pre-existing disparities tied to various factors, including race, ethnicity, religion, gender, disability, or sexual orientation. Therefore, to address the ongoing 'black box' problem and working towards developing more transparent and explainable AI models remain critical to fostering trust and acceptance among healthcare professionals[33].

Declaration of Competing Interest

The authors declare the following financial interests/personal relationships which may be considered as potential competing interests: Changbae Mun reports financial support was provided by National Research Foundation of Korea.

Acknowledgment

This research was supported by Basic Science Research Program through the National Research Foundation of Korea(NRF) funded by the Ministry of Education (2023S1A5A8078960).

References

[1] H. Fujita, AI-Based computer-Aided Diagnosis (AI-CAD): the latest review to read first, Radiol. Phys. Technol. 13 (1) (2020) 6–19, https://doi.org/10.1007/s12194-019-00552-4.
[2] Rikiya Yamashita, Mizuho Nishio, Richard K.G. DO, Kaori Togashi, Convolutional neural networks: an overview and application in radiology, Insights Imaging 9 (4) (2018) 611–629, https://doi.org/10.1007/s13244-018-0639-9.
[3] Yuan Yang, Lin Zhang, Mingyu Du, Jingyu Bo, Hao-Lei Liu, Lei Ren, Honggang Zhou, M.J. Deen, A comparative analysis of eleven neural networks architectures for small datasets of lung images of COVID-19 patients toward improved clinical decisions, Comput. Biol. Med. 139 (2021), 104887, https://doi.org/10.1016/j.compbiomed.2021.104887. December.
[4] Reed T. Sutton, David Pincock, D.C. Baumgart, Daniel C. Sadowski, Richard N. Fedorak, K.I. Kroeker, An overview of clinical decision support systems: benefits, risks, and strategies for success, NPJ Digit. Med. 3 (1) (2020), https://doi.org/10.1038/s41746-020-0221-y.
[5] Yogesh Kumar, Apeksha Koul, Ruchi Singla, M. Ijaz, Artificial intelligence in disease diagnosis: a systematic literature review, synthesizing framework and future research agenda, J. Ambient Intell. Humaniz. Comput. (2022), https://doi.org/10.1007/s12652-021-03612-z. January.
[6] Wang, Shoujin, Wei Liu, Jia Wu, Longbing Cao, Qinxue Meng, and Paul J. Kennedy. 2016. Training deep neural networks on imbalanced data sets. 10.1109/ijcnn.2016.7727770.
[7] Yang Zhao, Zoie Shui-Yee Wong, Kwok-Leung Tsui, A framework of rebalancing imbalanced healthcare data for rare events' classification: a case of look-alike sound-alike mix-up incident detection, J. Healthc Eng. 2018 (2018) 1–11, https://doi.org/10.1155/2018/6275435. January.
[8] Masoud Abedi, Lars Hempel, Sina Sadeghi, Toralf Kirsten, GAN-based approaches for generating structured data in the medical domain, Appl. Sci. 12 (14) (2022) 7075, https://doi.org/10.3390/app12147075.
[9] Weijun Cheng, Tengfei Ma, Xiaoting Wang, Gang Wang, Anomaly detection for internet of things time series data using generative adversarial networks with attention mechanism in smart agriculture, Front Plant Sci. 13 (2022), https://doi.org/10.3389/fpls.2022.890563. June.
[10] D. Castelvecchi, Can we open the black box of AI? Nature 538 (7623) (2016) 20–23, https://doi.org/10.1038/538020a.
[11] Julia Amann, Effy Vayena, Dietmar Frey, V.I. Madai, Explainability for artificial intelligence in healthcare: a multidisciplinary perspective, BMC Med. Inform. Decis. Mak. 20 (1) (2020), https://doi.org/10.1186/s12911-020-01332-6.
[12] Sagar Kora Venu, Sridhar Ravula, Evaluation of deep convolutional generative adversarial networks for data augmentation of chest x-ray images, Fut. Int. 13 (1) (2020) 8, https://doi.org/10.3390/fi13010008.
[13] Adnan Saood, Iyad Hatem, COVID-19 Lung CT image segmentation using deep learning methods: u-net versus SegNet, BMC Med. Imaging 21 (1) (2021), https://doi.org/10.1186/s12880-020-00529-5.
[14] Ian Goodfellow, Jean Pouget-Abadie, Mehdi Mirza, Bing Xu, David Warde-Farley, Sherjil Ozair, Aaron Courville, Yoshua Bengio, Generative adversarial networks, Commun. ACM 63 (11) (2020) 139–144, no.
[15] Thomas Schlegl, Philipp Seeböck, Sebastian M Waldstein, Ursula Schmidt-Erfurth, Georg Langs, Unsupervised anomaly detection with generative adversarial networks to guide marker discovery. Lecture Notes in Computer Science, Springer Science+Business Media, 2017, pp. 146–157, https://doi.org/10.1007/978-3-319-59050-9_12.
[16] Radford, Alec, Luke Metz, and Soumith Chintala. "Unsupervised representation learning with deep convolutional generative adversarial networks." arXiv preprint arXiv:1511.06434 (2015).
[17] Saman Motamed, Patrik Rogalla, Farzad Khalvati, Data augmentation using generative adversarial networks (GANs) for GAN-based detection of pneumonia and COVID-19 in Chest X-Ray Images, Inform. Med. Unlock. 27 (2021), 100779, https://doi.org/10.1016/j.imu.2021.100779. January.
[18] Christian Ledig, Lucas Theis, Ferenc Huszár, Jose Caballero, Andrew Cunningham, Alejandro Acosta, Andrew Aitken, et al., Photo-realistic single image super-resolution using a generative adversarial network, in: Proceedings of the IEEE Conference on Computer Vision and Pattern Recognition, 2017, pp. 4681–4690.
[19] M. Cheon, SR-AnoGAN: you never detect alone. super resolution in anomaly detection (Student Abstract), in: Proceedings of the AAAI Conference on Artificial Intelligence 37, 2023, pp. 16194–16195, https://doi.org/10.1609/aaai.v37i13.26957.
[20] Changyong Li, Yong-Xian Fan, Xiaodong Cai, PyConvU-Net: a lightweight and multiscale network for biomedical image segmentation, BMC Bioinformat. 22 (1) (2021), https://doi.org/10.1186/s12859-020-03943-2.
[21] Olaf Ronneberger, Philipp Fischer, Thomas Brox, U-Net: convolutional Networks for Biomedical Image Segmentation. Lecture Notes in Computer Science, Springer Science+Business Media, 2015, pp. 234–241, https://doi.org/10.1007/978-3-319-24574-4_28.
[22] "COVID19_Pneumonia_Normal_Chest_Xray_PA_Dataset." 2020. Kaggle. July 13, 2020. https://www.kaggle.com/datasets/amanullahasraf/covid19-pneumonia-normal-chest-xray-pa-dataset?select=covid.
[23] "Chest Xray masks and labels." 2019. Kaggle. January 21, 2019. https://www.kaggle.com/datasets/nikhilpandey360/chest-xray-masks-and-labels.
[24] Xiaolong Pei, Yuhong Zhao, Long-Qing Chen, Qingwei Guo, Zhiqiang Duan, Yue Pan, Hua Hou, Robustness of machine learning to color, size change, normalization, and image enhancement on micrograph datasets with large sample differences, Mater. Des. 232 (2023), 112086, https://doi.org/10.1016/j.matdes.2023.112086. August.
[25] Andre. Ye, Modern Deep learning design and application development, Apress EBooks (2022), https://doi.org/10.1007/978-1-4842-7413-2.
[26] Z. Ren, X. Kong, Y. Zhang, S. Wang, UKSSL: underlying knowledge based semi-supervised learning for medical image classification, IEEE Open J. Eng. Med. Biol. (2023).
[27] Y. Zhang, L. Deng, H. Zhu, W. Wang, Z. Ren, Q. Zhou, S. Wang, Deep learning in food category recognition, Inform. Fusion (2023), 101859.
[28] S. Dramburg, M.L. Fernández, E. Potapova, P.M. Matricardi, The Potential of clinical decision support systems for prevention, diagnosis, and monitoring of allergic diseases, Front. Immunol. 11 (2020), https://doi.org/10.3389/fimmu.2020.02116.
[29] M. Laka, A. Milazzo, T. Merlin, Factors that impact the adoption of clinical decision support systems (CDSS) for antibiotic management, Int. J. Environ. Res. Public Health 18 (4) (2021) 1901, https://doi.org/10.3390/ijerph18041901.
[30] F. Valente, S. Paredes, J. Henriques, T. Rocha, P. De Carvalho, J. Morais, Interpretability, personalization and reliability of a machine learning based clinical decision support system, Data Min. Knowl. Discov. 36 (3) (2022) 1140–1173, https://doi.org/10.1007/s10618-022-00821-8.
[31] C. Castaneda, K. Nalley, C. Mannion, P.K. Bhattacharyya, P.S. Blake, A.L. Pecora, A. Goy, K. Suh, Clinical decision support systems for improving diagnostic accuracy and achieving precision medicine, J. Clin. Bioinforma. 5 (1) (2015), https://doi.org/10.1186/s13336-015-0019-3.
[32] S. Dash, S.K. Shakyawar, M. Sharma, S. Kaushik, Big data in healthcare: management, analysis and future prospects, J. Big Data 6 (1) (2019), https://doi.org/10.1186/s40537-019-0217-0.
[33] M. Mittermaier, M.M. Raza, J.C. Kvedar, Bias in AI-based models for medical applications: challenges and mitigation strategies, NPJ Digit. Med. 6 (1) (2023), https://doi.org/10.1038/s41746-023-00858-z.